Neural Path Features and Neural Path Kernel : Understanding the role of gates in deep learning

Anonymous Author(s)
Affiliation
Address
email

Abstract

Rectified linear unit (ReLU) activations can also be thought of as *gates*, which, either pass or stop their pre-activation input when they are *on* (when the pre-activation input is positive) or *off* (when the pre-activation input is negative) respectively. A deep neural network (DNN) with ReLU activations has many gates, and the on/off status of each gate changes across input examples as well as network weights. For a given input example, only a subset of gates are *active*, i.e., on, and the sub-network of weights connected to these active gates is responsible for producing the output. At randomised initialisation, the active sub-network corresponding to a given input example is random. During training, as the weights are learnt, the active sub-networks are also learnt, and potentially hold very valuable information.

In this paper, we analytically characterise the role of active sub-networks in deep learning. To this end, we encode the on/off state of the gates of a given input in a novel *neural path feature* (NPF), and the weights of the DNN are encoded in a novel *neural path value* (NPV). Further, we show that the output of network is indeed the inner product of NPF and NPV. The main result of the paper shows that the *neural path kernel* associated with the NPF is a fundamental quantity that characterises the information stored in the gates of a DNN. We show via experiments (on MNIST and CIFAR-10) that in standard DNNs with ReLU activations NPFs are learnt during training and such learning is key for generalisation. Furthermore, NPFs and NPVs can be learnt in two separate networks and such learning also generalises well in experiments. In our experiments, we observe that almost all the information learnt by a DNN with ReLU activations is stored in the gates - a novel observation that underscores the need to further investigate the role of gating in DNNs.

1 Introduction

We consider deep neural networks (DNNs) with rectified linear unit (ReLU) activations. A special property of ReLU activation is that it can be written as a product of its pre-activation input, say $q \in \mathbb{R}$ and a gating signal, $\gamma_r(q) = \mathbb{1}_{\{q>0\}}$, i.e., $\chi_r(q) = q \cdot \gamma_r(q)$. In what follows, we call χ_r as the ReLU activation and γ_r as the ReLU gate. While the weights (of a DNN) remain the same across input examples, the $1/0$ state of the gates (or simply gates) change across input examples. For each input example, there is a corresponding *active* sub-network consisting of those gates which are 1, and the weights which pass through such gates. This active sub-network can be said to hold the memory for a given input, i.e., only those weights that pass through such active gates contribute to the output. In this viewpoint, at random initialisation of the weights, for a given input example, a random sub-network is active and produces a random output. However, as the weights change during training (say via gradient descent), the gates change, and hence the active sub-networks corresponding to the various input examples also change. At the end of training, for each input example, there is a learned active

38 sub-network, and produces a learned output. Thus, the gates of a trained DNN could potentially
39 contain valuable information. In this paper, we study the role of the gates, and the dynamics of the
40 gates while training DNNs using gradient descent (GD). Our findings can be summarised in the
41 following claims which we theoretically/experimentally justify in the paper:

42 Claim I (see Section 5): *Active sub-networks are fundamental entities in DNNs with ReLU activations.*

43 Claim II (see Section 6): *Learning of the active sub-networks during training is key for generalisation.*

44 Before we discuss "Claims I and II" in terms of our novel contributions in Section 1.2, we present the
45 background of *neural tangent feature and kernel* (NTF and NTK) in Section 1.1.

46 **Notation:** We denote the set $\{1, \ldots, n\}$ by $[n]$. For $x, y \in \mathbb{R}^m$, $\langle x, y \rangle = x^\top y$. The maximum
47 and minimum eigenvalue of a real symmetric matrix A are denoted by $\rho_{\max}(A)$ and $\rho_{\min}(A)$. We
48 consider fully-connected DNNs with w hidden units per layer and $d-1$ hidden layers. The output
49 of the DNN for an input $x \in \mathbb{R}^{d_{in}}$ is denoted by $\hat{y}_\Theta(x) \in \mathbb{R}$, where $\Theta \in \mathbb{R}^{d_{net}}$ are the network
50 weight ($d_{net} = d_{in}w + (d-2)w^2 + w$). We denote by $\Theta(l, j, i)$, the weight connecting the jth
51 hidden unit of layer $l - 1$ to the ith hidden unit of layer $l \in [d]$. $\Theta(1) \in \mathbb{R}^{w \times d_{in}}, \Theta(l) \in \mathbb{R}^{w \times w}, \forall l \in$
52 $\{2, \ldots, d-1\}, \Theta(d) \in \mathbb{R}^{w \times 1}$. The dataset is given by $(x_s, y_s)_{s=1}^n \in \mathbb{R}^{d_{in}} \times \mathbb{R}$. The loss function is
53 given by $L_\Theta = \frac{1}{2} \sum_{s=1}^n (\hat{y}_\Theta(x_s) - y_s)^2$. We use $\nabla_\Theta(\cdot)$ stands for the gradient of $(\cdot)$ with respect to
54 the network weights. We use vectorised notations $y = (y_s, s \in [n]), \hat{y}_\Theta = (\hat{y}_\Theta(x_s), s \in [n]) \in \mathbb{R}^n$
55 for the true and predicted outputs and $e_t = (\hat{y}_{\Theta_t} - y) \in \mathbb{R}^n$ for the error in the prediction. We use
56 $\theta \in \Theta$ to denote single arbitrary weight, and $\partial_\theta(\cdot)$ to denote $\frac{\partial(\cdot)}{\partial\theta}$. $\Sigma \in \mathbb{R}^{n \times n}$ is the input Gram
57 matrix with entries $\Sigma(s, s') = \langle x_s, x_{s'} \rangle$.

1.1 Background: Neural Tangent Feature and Kernel

59 The NTF and NTK machinery was developed in some of the recent works [9, 1, 4, 6] to understand
60 optimisation and generalisation in DNNs trained using GD. For an input $x \in \mathbb{R}^{d_{in}}$, the NTF is given
61 by $\psi_{x,\Theta} = \nabla_\Theta \hat{y}_\Theta(x) \in \mathbb{R}^{d_{net}}$, i.e., the gradient of the network output with respect to its weights.
62 The NTK matrix K_Θ on the dataset is the $n \times n$ Gram matrix of the NTFs of the input examples, and
63 is given by $K_\Theta(s, s') = \langle \psi_{x_s, \Theta}, \psi_{x_{s'}, \Theta} \rangle, s, s' \in [n]$.

64 **Proposition 1.1** (**Lemma 3.1** Arora et al. [2019]). *Consider the GD procedure to minimise the*
65 *squared loss $L(\Theta)$ with infinitesimally small step-size: $\dot{\Theta}_t = -\nabla_\Theta L_{\Theta_t}$. If follows that the dynamics*
66 *of the error term can be written as $\dot{e}_t = -K_{\Theta_t} e_t$.*

67 **Prior works** [9, 6, 1, 4] have studied DNNs trained using GD in the so called 'NTK regime', which
68 occurs under appropriate randomised initialisation, and when the width of the DNN approaches
69 infinity. The characterising property of the NTK regime is that as $w \to \infty$, $K_{\Theta_0} \to K^{(d)}$, and
70 $K_{\Theta_t} \approx K_{\Theta_0}$, where $K^{(d)}$ (see (2) in Appendix A) is a deterministic matrix whose superscript (d)
71 denotes the depth of the DNN. Arora et al. [2019] show that infinite width DNN trained using
72 GD is equivalent to kernel regression with the limiting NTK matrix $K^{(d)}$ (and hence enjoys the
73 generalisation ability of the limiting NTK matrix $K^{(d)}$). Further, Arora et al. [2019] propose a pure
74 kernel method based on what they call the CNTK, which is the limiting NTK matrix $K^{(d)}$ for an
75 infinite width convolutional neural network (CNN). Cao and Gu [2019] show that in the NTK regime,
76 a DNN is almost a linear learner with the random NTFs at initialisation, and show a generalisation
77 bound in the form of $\tilde{\mathcal{O}}\left(d \cdot \sqrt{y^\top (K^{(d)})^{-1} y/n}\right)$[1].

78 **Open Question:** Arora et al. [2019] report a $5\% - 6\%$ performance gain of finite width CNNs (which
79 do not operate in the NTK regime) over the exact CNTKs corresponding to infinite width CNNs, and
80 infer that the study of DNNs in the NTK regime cannot fully explain the success of practical neural
81 networks yet. Can we explain the reason for the performance gain of CNNs over CNTK?

---

[1]$a_t = \mathcal{O}(b_t)$ if $\limsup_{t \to \infty} |a_t/b_t| < \infty$, and $\tilde{\mathcal{O}}(\cdot)$ is used to hide logarithmic factors in $\mathcal{O}(\cdot)$.

1.2 Our Contributions

To the best of our knowledge, we are the first to analytically characterise the role played by active sub-networks in deep learning as presented in the 'Claims I and II'. The key contributions can be arranged into three landmarks as described below.

• The first step involves breaking a DNN into individual paths, and each path again into gates and weights. To this end, we encode the states of the gates in a novel *neural path feature* (NPF) and the weights in a novel *neural path value* (NPV) and express the output of the DNN as an inner product of NPF and NPV (see Section 2). In contrast to NTF/NTK which are *first-order* quantities (based on derivatives with respect to the weights), NPF and NPV are *zeroth-order* quantities. The kernel matrix associated to the NPFs namely the *neural path kernel* (NPK) matrix $H_\Theta \in \mathbb{R}^{n \times n}$ has a special structure, i.e., it can be written as a *Hadamard* product of the input Gram matrix, and a correlation matrix $\Lambda_\Theta \in \mathbb{R}^{n \times n}$, whose entries $\Lambda_\Theta(s, s')$ is equal to the total number of path in the sub-network that is active for both input examples $s, s' \in [n]$. With the Λ_Θ matrix we reach our first landmark.

• Second step is to characterise performance of active sub-networks in a 'stand alone' manner. To this end, we consider a new idealised setting namely fixed NPF (FNPF) setting, wherein, the NPFs are fixed (i.e., held constant) and only the NPV is learnt via gradient descent. In this setting, we show that (see Theorem 5.1), in the limit of infinite width and under randomised initialisation the NTK converges to a matrix $K_{\text{FNPF}}^{(d)} = \text{constant} \times H_{\text{FNPF}}$, where $H_{\text{FNPF}} \in \mathbb{R}^{n \times n}$ is the NPK matrix corresponding to the fixed NPFs. $K^{(d)}$ matrix of Jacot et al. [2018], Arora et al. [2019], Cao and Gu [2019] becomes the $K_{\text{FNPF}}^{(d)}$ matrix in the FNPF setting, wherein, we initialise the NPV statistically independent of the fixed NPFs (see Assumption 5.1). With Theorem 5.1, we reach our second landmark, i.e. we justify "Claim I", that active sub-networks are fundamental entities, which follows from the fact that $H_{\text{FNPF}} = \Sigma \odot \Lambda_{\text{FNPF}}$, where Λ_{FNFP} corresponds to the fixed NPFs.

• Third step is to show experimentally that sub-network learning happens in practice. We show that in finite width DNNs with ReLU activations, NPFs are learnt continuously during training, and such learning is key for generalisation. We observe that fixed NPFs obtained from the initial stages of training generalise poorly than CNTK (of Arora et al. [2019]), whereas, fixed NPFs obtained from later stages of training generalise better than CNTK and generalise as well as standard DNNs with ReLU. This throws light on the open question in Section 1.1, i.e., the difference between the NTK regime and the finite width DNNs is perhaps due to NPF learning. In finite width DNNs, NPFs are learnt during training and in the NTK regime no such feature learning happens during training (since $K^{(d)}$ is fixed). Since the NPFs completely encode the information pertaining to the active sub-networks, we complete our final landmark namely justification of "Claim II",

2 Neural Path Feature and Kernel: Encoding Gating Information

The gating property of the ReLU activation allows us to express the output of the DNN as a summation of the contribution of the individual paths, and paves a natural way to encode the $1/0$ states of the gates *without loss of information*. The contribution of a path is the product of the signal in its input node, the 'd' weights in the path and the '$(d-1)$' gates in the path. For an input $x \in \mathbb{R}^{d_{in}}$, and parameter $\Theta \in \mathbb{R}^{d_{net}}$, we encode the gating information in a novel *neural path feature* (NPF), $\phi_{x,\Theta} \in \mathbb{R}^P$ and the weights in a novel *neural path value* (NPV) $v_\Theta \in \mathbb{R}^P$, where, $P = d_{in}w^{(d-1)}$ is the total number of paths. The NPF co-ordinate of a path is the product of the signal at its input node and the gates in the path. The NPV co-ordinate of a path is the product of the weights in the paths. By stacking the NPFs of all the input examples we obtain the NPF matrix as $\Phi_\Theta = (\phi_{x_s,\Theta}, s \in [n]) \in \mathbb{R}^{P \times n}$. Then the input-output relationship of a DNN in vector form is given by:

$$\hat{y}_\Theta = \Phi_\Theta^\top v_\Theta, \tag{1}$$

where the NPF matrix Φ_Θ can also be interpreted as the *hidden feature matrix* which along with v_Θ is learnt during gradient descent on $\Theta \in \mathbb{R}^{d_{net}}$.

2.1 Paths, Neural Path Feature, Neural Path Value and Network Output

A path starts from an input node, passes through exactly one weight (and one hidden node) in each layer and ends at the output node. We have a total of $P = d_{in}w^{(d-1)}$ paths. Let us say that an

3

Input Layer	:	$z_{x,\Theta}(0)$	=	x
Pre-Activation	:	$q_{x,\Theta}(l,i)$	=	$\Theta(l,\cdot,i)^\top z_{x,\Theta}(l-1), l \in [d-1], i \in [w]$
Gating Values	:	$G_{x,\Theta}(l,i)$	=	$\gamma_r(q_{x,\Theta}(l,i)), l \in [d-1], i \in [w]$, where $\gamma_r(q) = \mathbb{1}_{\{q>0\}}$
Hidden Layer	:	$z_{x,\Theta}(l,i)$	=	$\chi_r(q_{x,\Theta}(l,i)) = q_{x,\Theta}(l,i) \cdot G_{x,\Theta}(l,i), l \in [d-1], i \in [w]$
Final Output	:	$\hat{y}_\Theta(x)$	=	$\Theta(d)^\top z_{x,\Theta}(d-1)$

Table 1: DNN with ReLU activation. Here, $x \in \mathbb{R}^{d_{in}}$ is the input to the DNN, and $\hat{y}_\Theta(x)$ is the output, 'q's are pre-activation inputs, 'z's are output of the hidden layers, 'G's are the gating values. $l \in [d-1]$ is the index of the layer, and $i \in [w]$ is the index of the hidden units in a layer.

enumeration of the paths is given by $[P] = \{1,\ldots,P\}$. Let $\mathcal{I}_l \colon [P] \to [w], l = 0, \ldots, d-1$ provide the index of the hidden unit through which a path p passes in layer l (with the convention that $\mathcal{I}_d(p) = 1, \forall p \in [P]$).

Definition 2.1. *Let $x \in \mathbb{R}^{d_{in}}$ be the input to the DNN. For this input,*

(i) The activity of a path p is given by : $A_\Theta(x,p) \overset{def}{=} \Pi_{l=1}^{d-1} G_{x,\Theta}(l, \mathcal{I}_l(p))$.

(ii) The neural path feature (NPF) is given by : $\phi_{x,\Theta} \overset{def}{=} (x(\mathcal{I}_0(p)) A_\Theta(x_s, p), p \in [P]) \in \mathbb{R}^P$.

(iii) The neural path value (NPV) if given by : $v_\Theta \overset{def}{=} \left(\Pi_{l=1}^d \Theta(l, \mathcal{I}_{l-1}(p), \mathcal{I}_l(p)), p \in [P]\right) \in \mathbb{R}^P$.

A path p is active if all the gates in the paths are on.

Proposition 2.1. *The output of the network can be written as an inner product of the NPF and NPV, i.e.,* $\hat{y}_\Theta(x) = \langle \phi_{x,\Theta}, v_\Theta \rangle = \sum_{p \in [P]} x(\mathcal{I}_0(p)) A_\Theta(x,p) v_\Theta(p)$.

$$\phi_{x_1} = [0,0,x_1(1),0,0,0,0,0,x_1(1),0,0,x_1(2),0,0,0,0,0,x_1(2)]^\top$$
$$\phi_{x_2} = [0,x_2(1),x_2(1),0,0,0,0,0,0,0,x_2(2),x_2(2),0,0,0,0,0,0]^\top \quad , \Lambda = \begin{bmatrix} 2 & 1 & 0 \\ 1 & 2 & 0 \\ 0 & 0 & 2 \end{bmatrix}$$
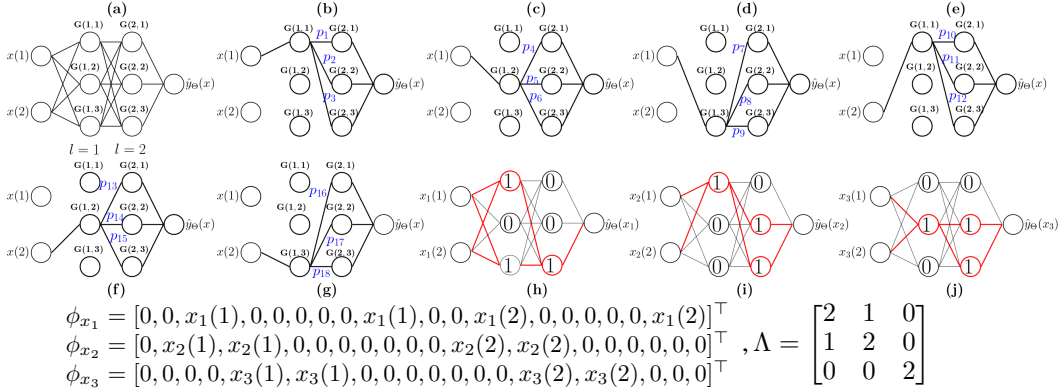$$\phi_{x_3} = [0,0,0,0,x_3(1),x_3(1),0,0,0,0,0,0,0,0,x_3(2),x_3(2),0,0,0]^\top$$

Figure 1: A toy illustration of gates, paths and active sub-networks. The cartoon (**a**) in the top left corner shows a DNN with 2 hidden layers, 6 ReLU gates $G(l,i), l = 1,2, i = 1,2,3$, 2 input nodes $x(1)$ and $x(2)$ and an output node $\hat{y}_\Theta(x)$. Cartoons (**b**) to (**g**) show the enumeration of the paths $p_1, \ldots, p_{18}$. Cartoons (**h**), (**i**) and (**j**) show hypothetical gates for 3 different hypothetical input examples $\{x_s\}_{s=1}^3 \in \mathbb{R}^2$. In each of the cartoons (**h**), (**i**) and (**j**), the $1/0$ inside the circles denotes the on/off state of the gates, and the bold paths/gates shown in red colour constitute the active sub-network for that particular input example. The NPFs are given by $\phi_x = [x(1)A(x,p_1), \ldots, x(1)A(x,p_9), x(2)A(x,p_{10}), \ldots, x(2)A(x,p_{18})]^\top$. Here, $\Lambda(1,2) = 1$ because paths p_3 and p_{12} are both active for input examples x_1 and x_2 and the input dimension is 2.

2.2 Neural Path Kernel : Similarity based on active sub-networks

Definition 2.2. *For input examples $s, s' \in [n]$, define $\mathcal{A}_\Theta(s,s') \overset{def}{=} \{p \in [P] \colon A_\Theta(x_s,p) = A_\Theta(x_{s'},p) = 1\}$ to be the set of 'active' paths for both s, s' and $\Lambda_\Theta(s,s') \overset{def}{=} \frac{|\mathcal{A}_\Theta(s,s')|}{d_{in}}$.*

Remark: Owing to the symmetry of a DNN, the same number of active paths start from any fixed input node. In Definition 2.2, Λ_Θ measures the size of the active sub-network as the total number of

active paths starting from any fixed input node. For examples $s, s' \in [n], s \neq s'$, $\Lambda_\Theta(s,s)$ is equal to the size of the sub-network active for s, and $\Lambda_\Theta(s,s')$ is equal to the size of the sub-network active for both s and s'. For an illustration of NPFs and Λ please see Figure 1.

Lemma 2.1. *Let $H_\Theta \stackrel{def}{=} \Phi_\Theta^\top \Phi_\Theta$ be the NPK matrix, and $\Lambda_\Theta \in \mathbb{R}^{n \times n}$ be as in Definition 2.2 . It follows that $H_\Theta = \Sigma \odot \Lambda_\Theta$, where $\odot$ is the Hadamard product, and Σ is the input Gram matrix.*

3 Dynamics of Gradient Descent with NPF and NPV Learning

In Section 2, we mentioned that during gradient descent, the DNN is learning a relation $\hat{y}_\Theta = \Phi_\Theta^\top v_\Theta$, i.e., both the NPFs and the NPV are learnt. In this section, we connect the newly defined quantities, i..e, Φ_Θ and v_Θ to the NTK matrix K_Θ (see Proposition 3.1), and re-write the gradient descent dynamics in Proposition 3.2 taking into account of NPF and NPV learning.

3.1 NPV and NPF Learning

Definition 3.1. *The gradient of the NPV of path p is defined as $\varphi_{p,\Theta} \stackrel{def}{=} (\partial_\theta v_\Theta(p), \theta \in \Theta) \in \mathbb{R}^{d_{net}}$.*

Remark The change of the NPV is given by $\dot{v}_{\Theta_t}(p) = \langle \varphi_{p,\Theta_t}, \dot{\Theta}_t \rangle$, where $\dot{\Theta}_t$ is the change of the weights. We now collect the gradients $\varphi_{p,\Theta}$ of all the paths to define a *value tangent kernel* (VTK).

Definition 3.2. *Let $\nabla_\Theta v_\Theta$ be a $d_{net} \times P$ matrix of NPV derivatives given by $\nabla_\Theta v_\Theta = (\varphi_{p,\Theta}, p \in [P])$. Define the VTK to be the $P \times P$ matrix given by $\mathcal{V}_\Theta = (\nabla_\Theta v_\Theta)^\top (\nabla_\Theta v_\Theta)$.*

Remark An important point to note here is that the VTK is a quantity that is dependent only on the weights. To appreciate the same, consider a deep linear network (DLN) [15, 5] which has identity activations, i.e., all the gates are 1 for all inputs, and weights. For a DLN and DNN with identical network architecture (i.e., w and d), and identical weights, $\mathcal{V}_\Theta$ is also identical. Thus, $\mathcal{V}_\Theta$ is the gradient based information that excludes the gating information.

The NPFs changes at those time instants when any one of the gates switches from 1 to 0 or from 0 to 1. In the time between two such switching instances, NPFs of all the input examples in the dataset remain the same, and between successive switching instances, the NPF of at least one of the input example in the dataset changes. In what follows, in Proposition 3.2 we re-write Proposition 1.1 taking into account the switching instances which we define in Definition 3.3.

Definition 3.3. *Define a sequence of monotonically increasing time instants $\{T_i\}_{i=0}^\infty$ (with $T_0 = 0$) to be 'switching' instants if $\phi_{x_s,\Theta_t} = \phi_{x_s,\Theta_{T_i}}, \forall s \in [n], \forall t \in [T_i, T_{i+1}), i = 0, \ldots, \infty$, and $\forall i = 0, \ldots, \infty \exists s(i) \in [n]$ such that $\phi_{x_{s(i)},\Theta_{T_i}} \neq \phi_{x_{s(i)},\Theta_{T_{i+1}}}$.*

3.2 Gradient Descent

Proposition 3.1. *The NTK is given by $K_\Theta = \Phi_\Theta^\top \mathcal{V}_\Theta \Phi_\Theta$.*

Remark K_{Θ_t} changes during training (i) continuously at all $t \geq 0$ due to $\mathcal{V}_{\Theta_t}$, and (ii) at switching instants $T_i, i = 0, \ldots, \infty$ due to the change in $\Phi_{\Theta_{T_i}}$. We now describe the gradient descent dynamics taking into the dynamics of the NPV and the NPFs.

Proposition 3.2. *Let $\{T_i\}_{i=0}^\infty$ be as in Definition 3.3. For $t \in [T_i, T_{i+1})$ and small step-size of GD:*

$$
\begin{array}{lllll}
\text{Weights Dynamics} & : & \dot{\Theta}_t & = & -\sum_{s=1}^n \psi_{x_s,\Theta_t} e_t(s) \\
\text{NPV Dynamics} & : & \dot{v}_{\Theta_t}(p) & = & \langle \varphi_{p,\Theta_t}, \dot{\Theta}_t \rangle, \forall p \in [P] \\
\text{Error Dynamics} & : & \dot{e}_t & = & -K_{\Theta_t} e_t, \text{ where } K_{\Theta_t} = \Phi_{\Theta_{T_i}}^\top \mathcal{V}_{\Theta_t} \Phi_{\Theta_{T_i}}
\end{array}
$$

Proposition 3.3. $\rho_{min}(K_\Theta) \leq \rho_{\min}(H_\Theta) \rho_{\max}(\mathcal{V}_\Theta)$.

Remark For the NTK to be well conditioned, it is necessary for the NPK to be well conditioned. This is quite intuitive, in that, the closer two inputs are, the closer are their NPFs, and it is harder to train the network to produce arbitrarily different outputs for such inputs that are very close to one another.

5

4 Deep Gated Networks: Decoupling Neural Path Feature and Value

In order to ascertain that NPF learning indeed makes a difference, we should measure the generalisation performance with and without NPF learning. This can be achieved by a deep gated network (see Figure 2 below for details) having two networks of identical architecture namely i) a feature network parameterised by $\Theta^F \in \mathbb{R}^{d_{net}}$, that holds gating information, and hence the NPFs and ii) a value network that holds the NPVs parameterised by $\Theta^V \in \mathbb{R}^{d_{net}}$. In what follows, we let $\Theta^{DGN} = (\Theta^F, \Theta^V) \in \mathbb{R}^{2d_{net}}$ to denote the combined parameters of a DGN. By making $\Theta^F \in \mathbb{R}^{d_{net}}$ trainable/non-trainable, we can *enable/disable* the NPF gradient, which gives rise to the following two modes of operating a DGN:

1. **Fixed NPF (FNPF):** Here, $\Theta^F_t = \Theta^F_0, \forall t \geq 0$, i.e., $\Theta^F \in \mathbb{R}^{d_{net}}$ is non-trainable. Thus the DGN learns the relation $\hat{y}_{\Theta^{DGN}} = \Phi^\top_{\Theta^F_0} v_{\Theta^V}$, where $\Phi_{\Theta^F_0} \in \mathbb{R}^{P \times n}$ is a fixed NPF matrix, and v_{Θ^V} is learned via gradient descent on $\Theta^V \in \mathbb{R}^{d_{net}}$.

2. **Decoupled NPF Learning (DNPFL):** Here both $\Theta^F \in \mathbb{R}^{d_{net}}$ and $\Theta^V \in \mathbb{R}^{d_{net}}$ are trained, and the DGN learns the relation $\hat{y}_{\Theta^{DGN}} = \Phi^\top_{\Theta^F} v_{\Theta^V}$. In comparison to (1), here we have two parameters $\Theta^F \in \mathbb{R}^{d_{net}}$ and $\Theta^V \in \mathbb{R}^{d_{net}}$ as opposed to a single $\Theta \in \mathbb{R}^{d_{net}}$ in (1).

Note: FNPF and DNPFL are idealised modes to understand the role of gates, and not alternate proposals to replace standard DNNs with ReLU activations.
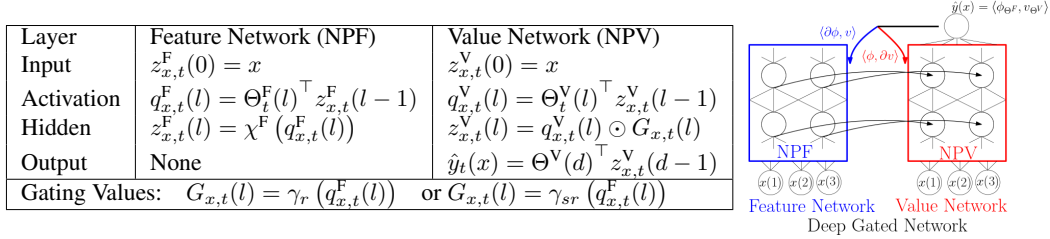

Layer	Feature Network (NPF)	Value Network (NPV)
Input	$z^F_{x,t}(0) = x$	$z^V_{x,t}(0) = x$
Activation	$q^F_{x,t}(l) = \Theta^F_t(l)^\top z^F_{x,t}(l-1)$	$q^V_{x,t}(l) = \Theta^V_t(l)^\top z^V_{x,t}(l-1)$
Hidden	$z^F_{x,t}(l) = \chi^F\left(q^F_{x,t}(l)\right)$	$z^V_{x,t}(l) = q^V_{x,t}(l) \odot G_{x,t}(l)$
Output	None	$\hat{y}_t(x) = \Theta^V(d)^\top z^V_{x,t}(d-1)$
Gating Values:	$G_{x,t}(l) = \gamma_r\left(q^F_{x,t}(l)\right)$ or $G_{x,t}(l) = \gamma_{sr}\left(q^F_{x,t}(l)\right)$	

Figure 2: Deep gated network (DGN) setup. The pre-activations $q^F_{x,t}(l)$ of layer $l \in [d-1]$ from the feature network are used to derive the gating values $G_{x,t}(l)$ of layer $l \in [d-1]$.

Proposition 4.1 (Gradient Dynamics in a DGN). *Let* $\psi^F_{x,\Theta^{DGN}} \stackrel{def}{=} \nabla_{\Theta^F} \hat{y}_{\Theta^{DGN}}(x) \in \mathbb{R}^{d_{net}}$, $\psi^V_{x,\Theta^{DGN}} \stackrel{def}{=} \nabla_{\Theta^V} \hat{y}_{\Theta^{DGN}}(x) \in \mathbb{R}^{d_{net}}$. *Let* $K^V_{\Theta^{DGN}}$ *and* $K^F_{\Theta^{DGN}}$ *be* $n \times n$ *matrices with entries* $K^V_{\Theta^{DGN}}(s, s') = \langle \psi^V_{x_s,\Theta^{DGN}}, \psi^V_{x_{s'},\Theta^{DGN}} \rangle$ *and* $K^F_{\Theta^{DGN}}(s, s') = \langle \psi^F_{x_s,\Theta^{DGN}}, \psi^F_{x_{s'},\Theta^{DGN}} \rangle$. *For infinitesimally small step-size of GD, the error dynamics in a DGN (in the DNPFL and FNPF modes) is given by:*

Dynamics	DNPFL		FNPF
Weight	$\dot{\Theta}^V_t$	$= -\sum_{s=1}^n \psi^V_{x,\Theta^{DGN}_t} e_t(s), \dot{\Theta}^F_t = -\sum_{s=1}^n \psi^F_{x,\Theta^{DGN}_t} e_t(s)$	$\dot{\Theta}^V_t$ same as (DNFPL), $\dot{\Theta}^F_t = 0$
NPF	$\dot{\phi}_{x_s,\Theta^F_t}(p)$	$= x(\mathcal{I}_0(p)) \sum_{\theta^F \in \Theta^F} \partial_{\theta^F} A_{\Theta^F_t}(x_s, p) \dot{\theta}^F_t, \forall p \in [P], s \in [n]$	$\dot{\phi}_{x_s,\Theta^F_t}(p) = 0$
NPV	$\dot{v}_{\Theta^V_t}(p)$	$= \sum_{\theta^V \in \Theta^V} \partial_{\theta^V} v_{\Theta^V_t}(p) \dot{\theta}^V_t, \forall p \in [P]$	$\dot{v}_{\Theta^V_t}(p)$ same as DNPFL
Error	$\dot{e}_t$	$= -\left(K^V_{\Theta^{DGN}} + K^F_{\Theta^{DGN}}\right) e_t$	$\dot{e}_t = -\left(K^V_{\Theta^{DGN}}\right) e_t$

Remark: The gradient dynamics in a DGN specified in Proposition 4.1 is similar to the gradient dynamics in a DNN specified in Proposition 3.2. Important difference is that in a DGN there are $2d_{net}$ parameters, and hence the NTF $\psi_{x,\Theta} = (\psi^F_{x,\Theta}, \psi^V_{x,\Theta}) \in \mathbb{R}^{2d_{net}}$, wherein, $\psi^V_{x,\Theta^{DGN}} \in \mathbb{R}^{d_{net}}$ flows through the value network and $\psi^F_{x,\Theta^{DGN}} \in \mathbb{R}^{d_{net}}$ flows through the feature network.

5 Learning with Fixed NPFs: Role Of Active Sub-Networks

In this section, we provide theoretical justification for "Claim I", i.e., the active sub-networks are fundamental entities in DNNs.

Definition 5.1. *Define the measure of information stored in the gates of a* DNN *with parameter* $\bar{\Theta} \in \mathbb{R}^{d_{net}}$ *to be the generalisation performance of a* DGN *with identical architecture operated in the* FNPF *mode whose* $\Theta^F_0 = \bar{\Theta}$ *are non-trainable, and* $\Theta^V \in \mathbb{R}^{d_{net}}$ *are trained.*

217 Consider a DNN parameterised by $\bar{\Theta} \in \mathbb{R}^{d_{net}}$. At randomised initialisation, we can obtain random
218 NPFs $\Phi_{\bar{\Theta}_0}$, and after training for T epochs, and we can obtain learnt NPFs $\Phi_{\bar{\Theta}_T}$. Thus, while
219 measuring information in the gates of this trained DNN, as per Definition 5.1, we are retaining $\Phi_{\bar{\Theta}_T}$
220 by storing the weights as $\Theta_0^{\mathrm{F}} = \bar{\Theta}_T$ in the feature network, and discarding $v_{\bar{\Theta}_T}$, and re-training Θ^{V}
221 to learn a new relation $\hat{y}_{\Theta^{\mathrm{DGN}}} = \Phi_{\Theta_0^{\mathrm{F}}}^{\top} v_{\Theta^{\mathrm{V}}} = \Phi_{\bar{\Theta}_T}^{\top} v_{\Theta^{\mathrm{V}}}$. Similarly, in the case of random NPFs we are
222 learning the relation, $\hat{y}_{\Theta^{\mathrm{DGN}}} = \Phi_{\Theta_0^{\mathrm{F}}}^{\top} v_{\Theta^{\mathrm{V}}} = \Phi_{\bar{\Theta}_0}^{\top} v_{\Theta^{\mathrm{V}}}$. In what follows, we use H_{FNFP} to refer to $H_{\Theta_0^{\mathrm{F}}}$.

223 **Assumption 5.1.** *(i) $\Theta_0^V \in \mathbb{R}^{d_{net}}$ is statistically independent of the fixed NPFs (stored in $\Theta_0^F \in \mathbb{R}^{d_{net}}$*
224 *of the feature network), (ii) Θ_0^V are sampled i.i.d from symmetric Bernoulli over $\{-\sigma, +\sigma\}$.*

225 **Theorem 5.1.** *Under Assumption 5.1, as $w \to \infty$, $K_{\Theta_0^{DGN}} \to K_{FNPF}^{(d)} = d \cdot \sigma^{2(d-1)} H_{FNPF}$.*

226 • **Active Sub-Network:** From previous results Arora et al. [2019], it follows that as $w \to \infty$, the
227 optimisation and generalisation properties of the fixed NPF learner can be tied down to the infinite
228 width NTK of the FNPF learner $K_{\mathrm{FNPF}}^{(d)}$ and hence to H_{FNPF} (treating $d\sigma^{2(d-1)}$ as a scaling factor).
229 We can further breakdown $H_{\mathrm{FNPF}} = \Sigma \odot \Lambda_{\mathrm{FNPF}}$, where $\Lambda_{\mathrm{FNPF}} = \Lambda_{\Theta_0^{\mathrm{F}}}$. This justifies "Claim I".

230 • $K^{(d)}$ in prior works [9, 1, 4] essentially becomes $K_{\mathrm{FNPF}}^{(d)}$ under Assumption 5.1. To understand
231 this, let us consider a DNN with weights $\Theta \in \mathbb{R}^{d_{net}}$. From [9, 1, 4] it follows that under randomised
232 initialisation of $\Theta_0 \in \mathbb{R}^{d_{net}}$ as $w \to \infty$ the NTK of the DNN $K_{\Theta_0} \to K^{(d)}$. The simplification
233 of $K^{(d)}$ to $K_{\mathrm{FNPF}}^{(d)}$ in Theorem 5.1 occurs when we copy these random NPFs corresponding to
234 $\Theta_0 \in \mathbb{R}^{d_{net}}$ into the feature network and keep them fixed, i.e., $\Theta_t^{\mathrm{F}} = \Theta_0^{\mathrm{F}} = \Theta_0 \in \mathbb{R}^{d_{net}}, t \geq 0$, and
235 train $\Theta^{\mathrm{V}} \in \mathbb{R}^{d_{net}}$ with initialisation as per Assumption 5.1.

236 • **Choice of σ:** In the case of random NPFs obtained by initialising Θ_0^{F} at random by sampling from a
237 symmetric distribution, we expect $\frac{w}{2}$ gates to be on every layer, so $\sigma = \sqrt{\frac{2}{w}}$ is a normalising choice,
238 in that, the diagonal entries of $\sigma^{2(d-1)} \Lambda_{\mathrm{FNPF}}(s, s) \approx 1$ in this case.

239 • We discuss a more detailed version of Theorem 5.1 in the Appendix, where we discuss the role of
240 width and depth on a pure memorisation task.

6 Experiments: Fixed NPFs, NPF Learning and Verification of Claim II

242 In this section, we justify "Claim II", i.e., active sub-networks learning is key for generalisation.
243 Since the active sub-network are encoded in the NPFs, we verify the claim by comparing different
244 network settings which vary in their NPF learning capabilities. We resolve the open question of Arora
245 et al. [2019] mentioned in Section 1.1, by providing an empirical explanation for the performance
246 gain of finite width CNN over the pure kernel method based on the exact infinite width CNTK.
247 **Networks for Comparison:** The performance of the following networks on standard MNIST and
248 CIFAR-10 datasets will be used for comparison: (i) fixed random (FRNPF): in the DGN, we randomly
249 initialise both $\Theta_0^{\mathrm{F}}, \Theta_0^{\mathrm{V}}$, make Θ^{F} *non-trainable* and train only Θ^{V}, (ii) fixed learnt (FLNPF): we
250 initialise Θ_0^{V} randomly, and copy weights from a pre-trained ReLU network (of identical architecture)
251 into Θ_0^{F}. Similar to FR case, Θ^{F} is non-trainable and only Θ^{V} is trained (iii) decoupled learning
252 (DNPFL): we randomly initialise both $\Theta_0^{\mathrm{F}}, \Theta_0^{\mathrm{V}}$, and train both Θ^{F} and Θ^{V}, (iv) ReLU: Standard
253 DNNs/CNNs with ReLU. We will also use the numerical results reported in Arora et al. [2019].
254 1. **Finite Vs Infinite width alone is not enough to explain the performance gain of CNN:** Both
255 FRNPF and ReLU are finite width networks. However, performance of FRNPF is approximately 67%
256 which is worse than CNTK of Arora et al. [2019] whose performance is 77.43%, and the performance
257 of our CNN architecture with *global-average-pooling* (GCONV in Table 2) is 80.34%. We trained
258 FRNPF with independent initialisation (II), where Θ_0^{F} and Θ_0^{V} are statistically independent, and
259 dependent initialisation (DI), where $\Theta_0^{\mathrm{F}} = \Theta_0^{\mathrm{V}}$. FRNPF (II) and FRNPF (DI) were close in our
260 experiments (see columns 4 and 5 in Table 2). Further, both FRNPF (DI) and ReLU start with the
261 same NTK matrix at initialisation. If finite width was the sole reason for the better performance then
262 even FRNPF (II), (DI) should have performed better than CNTK in the experiments, and they did not.
263 Thus, finite width alone does not explain the performance gain of CNN over CNTK.
264 2. **NPF Learning Vs No NPF Learning is key to explain the performance gain of CNN:** FLNPF
265 with weights copied from a fully trained ReLU performs close to 79.68% which is almost as good
266 as ReLU's 80.43% (see FLNP column in Table 2). Further, NPFs are learnt continuously during
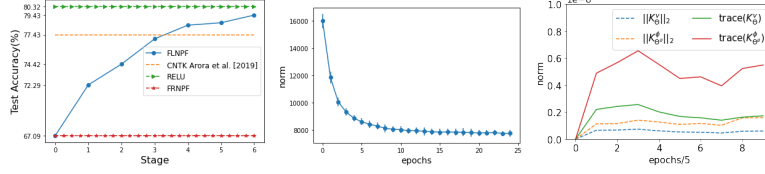
7

Figure 3: Dynamics of NPF Learning.

Arch	Optimiser	Dataset	FRNPF (II)	FRNPF (DI)	DNPFL	FLNPF	ReLU
FC	SGD	MNIST	95.85 ± 0.10	95.85 ± 0.17	97.86 ± 0.11	97.10 ± 0.09	97.85 ± 0.09
FC	Adam	MNIST	96.02 ± 0.13	96.09 ± 0.12	$\mathbf{98.22 \pm 0.05}$	97.82 ± 0.02	$\mathbf{98.14 \pm 0.07}$
VCONV	SGD	CIFAR-10	58.92 ± 0.62	58.83 ± 0.27	63.21 ± 0.07	63.06 ± 0.73	67.02 ± 0.43
VCONV	Adam	CIFAR-10	64.86 ± 1.18	64.68 ± 0.84	$\mathbf{69.45 \pm 0.76}$	$\mathbf{71.4 \pm 0.47}$	$\mathbf{72.43 \pm 0.54}$
GCONV	SGD	CIFAR-10	67.36 ± 0.56	66.86 ± 0.44	74.57 ± 0.43	78.52 ± 0.39	78.90 ± 0.37
GCONV	Adam	CIFAR-10	67.09 ± 0.58	67.08 ± 0.27	$\mathbf{77.12 \pm 0.19}$	$\mathbf{79.68 \pm 0.32}$	$\mathbf{80.43 \pm 0.35}$

Table 2: Shows the generalisation performance of different NPFs learning settings. The values in the table are averaged over 5 runs. Here, FC is a fully connected network with $w = 100$ and $d = 5$. VCONV and GCONV denote Vanilla CNN and CNN with GAP respectively. Please check Appendix B for details on architecture of VCONV and GCONV, and the hyper-parameters.

the training, and the performance gap between FRNPF and ReLU is continuous. In the case of CIFAR-10, we trained a GCONV network (parameterised by $\bar{\Theta}$) for 60 epochs, and we obtained 6 different weights at various *stages* of the training process. Stage 1: $\bar{\Theta}_{10}$, stage 2: $\bar{\Theta}_{20}$, stage 3: $\bar{\Theta}_{30}$, stage 4: $\bar{\Theta}_{40}$, stage 5: $\bar{\Theta}_{50}$, stage 6: $\bar{\Theta}_{60}$. We copy these weights obtained at various stages of training to setup 6 different FLNPFs, i.e., FLNPF-1 to FLNPF-6. We observe that the performance of FLNPF-1 to FLNPF-6 increases monotonically, with FLNPF-1 performing 72% which is better than FRNPF (i.e., 67.08%), and FLNPF-6 performing as well as ReLU (see left most plot in Figure 3). The performance of CNTK of Arora et al. [2019] is 77.43%. Thus, through its various stages, the FLNPF starts from below 77.43% and surpasses to reach 79.68%, which implies performance gain of CNN is due to learning of NPFs.

3. **Dynamics of active sub-networks during training:** We considered "Binary"-MNIST data set with two classes namely digits 4 and 7, with the labels taking values in $\{-1, +1\}$ and squared loss. We trained a fully connected (FC) network ($w = 100$, $d = 5$). Let $\widehat{H}_{\Theta_t} = \frac{1}{trace(H_{\Theta_t})} H_{\Theta_t}$ be the normalised NPK matrix. For a subset size, $n' = 200$ (100 examples per class) we plot $\nu_t = y^\top (\widehat{H}_{\Theta_t})^{-1} y$, (where $y \in \{-1, 1\}^{200}$ is the labelling function), and observe that ν_t reduces as training proceeds (see middle plot in Figure 3). Note that, $\nu_t = \sum_{i=1}^{n'} (u_{i,t}^\top y)^2 (\hat{\rho}_{i,t})^{-1}$, where $u_{i,t} \in \mathbb{R}^{n'}$ are the orthonormal eigenvectors of $\widehat{H}_{\Theta_t}$ and $\hat{\rho}_{i,t}, i \in [n']$ are the corresponding eigenvalues. Since $\sum_{i=1}^{n'} \hat{\rho}_{i,t} = 1$, the only way ν_t reduces is when more and more energy gets concentrated on $\hat{\rho}_{i,t}$s for which $(u_{i,t}^\top y)^2$s are also high. Since $H_{\Theta_t} = \Sigma \odot \Lambda_{\Theta_t}$, only Λ_{Θ_t} is learnt during training.

4. **Decoupled learning** of NPFs also performed better than FRNPFs (see column DNPFL in Table 2). This demonstrates the fact that NPFs can also be learnt in 'stand alone' manner. In this case, the NTK is given by $K_{\Theta^{DGN}} = K^V_{\Theta^{DGN}} + K^F_{\Theta^{DGN}}$. For MNIST, we compared $K^V_{\Theta^{DGN}}$ and $K^F_{\Theta^{DGN}}$ (calculated using 100 examples in total with 10 examples per each of the 10 classes) using their trace and Frobenius norms, and we observe that $K^V_{\Theta^{DGN}}$ and $K^F_{\Theta^{DGN}}$ are in the same scale (see right plot in Figure 3), which is perhaps pointing to the fact that both $K^F_{\Theta^{DGN}}$ and $K^F_{\Theta^{DGN}}$ are equally important for obtaining good generalisation performance. In DNPFL, we can separately study the kernel $K^F_{\Theta^{DGN}}$ responsible for NPF learning, an interesting future research direction.

7 Conclusion

In this paper, we studied the role of active sub-networks in deep learning by encoding the gates in the neural path features. We showed that the neural path features are learnt during training and such learning is key for generalisation. In our experiments, we observed that almost all information of a trained DNN is stored in the neural path features. We conclude by saying that *understanding deep learning requires understanding neural path feature learning*.

8

8   Broader Impact

Deep neural networks are still widely regarded as blackboxes. The standard and accepted view on the inner workings of deep neural networks is the 'layer-by-layer' viewpoint: as the input progresses through the hidden layers, features at different levels of abstractions are learnt. This paper deviates from the standard 'layer-by-layer' viewpoint, in that, it breaks down the deep neural network blackbox into its constituent paths: different set of paths get fired for different inputs, and the output is the summation of the contribution from individual paths. This makes the inner workings of deep neural networks interpretable, i.e., each input is remembered in terms of the active sub-network of the paths that get 'fired' for that input, and learning via gradient descent amounts to 'rewiring' of the paths. The paper also analytically connects this sub-network and path based view to the recent kernel based interpretation of deep neural networks, and furthers the understanding of feature learning in deep neural networks. We believe that these better insights into the working of DNNs can potentially lead to foundational algorithmic development in the future.

References

[1] Sanjeev Arora, Simon S Du, Wei Hu, Zhiyuan Li, Russ R Salakhutdinov, and Ruosong Wang. On exact computation with an infinitely wide neural net. In *Advances in Neural Information Processing Systems*, pages 8139–8148, 2019.

[2] Sanjeev Arora, Simon S Du, Wei Hu, Zhiyuan Li, and Ruosong Wang. Fine-grained analysis of optimization and generalization for overparameterized two-layer neural networks. *arXiv preprint arXiv:1901.08584*, 2019.

[3] Randall Balestriero et al. A spline theory of deep learning. In *International Conference on Machine Learning*, pages 374–383, 2018.

[4] Yuan Cao and Quanquan Gu. Generalization bounds of stochastic gradient descent for wide and deep neural networks. In *Advances in Neural Information Processing Systems*, pages 10835–10845, 2019.

[5] Simon S Du and Wei Hu. Width provably matters in optimization for deep linear neural networks. *arXiv preprint arXiv:1901.08572*, 2019.

[6] Simon S Du, Jason D Lee, Haochuan Li, Liwei Wang, and Xiyu Zhai. Gradient descent finds global minima of deep neural networks. *arXiv preprint arXiv:1811.03804*, 2018.

[7] Jonathan Fiat, Eran Malach, and Shai Shalev-Shwartz. Decoupling gating from linearity. *CoRR*, abs/1906.05032, 2019. URL http://arxiv.org/abs/1906.05032.

[8] Jonathan Frankle and Michael Carbin. The lottery ticket hypothesis: Finding sparse, trainable neural networks. *arXiv preprint arXiv:1803.03635*, 2018.

[9] Arthur Jacot, Franck Gabriel, and Clément Hongler. Neural tangent kernel: Convergence and generalization in neural networks. In *Advances in neural information processing systems*, pages 8571–8580, 2018.

[10] Arthur Jacot, Franck Gabriel, and Clément Hongler. Freeze and chaos for dnns: an ntk view of batch normalization, checkerboard and boundary effects. *arXiv preprint arXiv:1907.05715*, 2019.

[11] Jaehoon Lee, Lechao Xiao, Samuel Schoenholz, Yasaman Bahri, Roman Novak, Jascha Sohl-Dickstein, and Jeffrey Pennington. Wide neural networks of any depth evolve as linear models under gradient descent. In *Advances in neural information processing systems*, pages 8570–8581, 2019.

[12] Behnam Neyshabur, Russ R Salakhutdinov, and Nati Srebro. Path-sgd: Path-normalized optimization in deep neural networks. In *Advances in Neural Information Processing Systems*, pages 2422–2430, 2015.

[13] Vivek Ramanujan, Mitchell Wortsman, Aniruddha Kembhavi, Ali Farhadi, and Moham- mad Rastegari. What's hidden in a randomly weighted neural network? *arXiv preprint arXiv:1911.13299*, 2019.

[14] Andrew M Saxe, James L McClelland, and Surya Ganguli. Exact solutions to the nonlinear dynamics of learning in deep linear neural networks. *arXiv preprint arXiv:1312.6120*, 2013.

[15] Ohad Shamir. Exponential convergence time of gradient descent for one-dimensional deep linear neural networks. In *Conference on Learning Theory*, pages 2691–2713, 2019.

[16] Rupesh Kumar Srivastava, Jonathan Masci, Faustino Gomez, and Jürgen Schmidhuber. Under- standing locally competitive networks. *arXiv preprint arXiv:1410.1165*, 2014.